CFD MODELLING OF A NEGATIVELY BUOYANT PURGE FLOW IN THE BODY OF A REACTOR COOLANT CIRCULATOR

E Romero

on behalf of British Energy Generation Ltd

now at Rolls-Royce PLC, P.O. Box 3, Bristol BS34 7QE, UK

Abstract

The paper describes a finite element flow calculation using a two-equation turbulence model and variable properties, which analyses the effect of injecting a negatively buoyant flow stream into the primary circuit of a gas cooled reactor. This flow is intended to purge moisture laden gas from the compartment housing the electrical motors driving the primary circuit pumps. The study highlights the sensitivity to the use or otherwise of the Boussinesq approximation and the type of boundary conditions specified at the outlet of the calculational domain. The method of calculation was benchmarked against the challenging experiment on the mixing of stably stratified saline streams, as well as the higher order CFD modelling of the same experiment.

Introduction

Purging an undesired species from a process is not straightforward, as it may involve issues of instrumentation, control and confidence that the purge flow will achieve its purpose. One such instance involves a purging flow consisting of a negatively buoyant flow stream. Under some circumstances this may sink to the bottom of the passage or enclosure containing the process and thereby be rendered inactive or indeed generate a different set of problems.

The injection of dry pressurised CO_2 into the gas circulators of some gas cooled reactors has been considered in Britain to minimise the ingress of moisture laden pressurised CO_2 from the primary circuit into the compartment housing the electric motor of these circulators. The nature of the purging arrangement is such that the temperature of delivery may not be easily controlled. In supplying the CO_2, this may experience a significant isenthalpic expansion and therefore enter into the motor compartment at a significantly lower temperature than the gas already present there.

Thus, it is possible to generate a negatively buoyant stream which may sink towards the bottom of the compartment where it might not mix appreciably with the warmer gas and indeed may then impinge on internal components sensitive to low temperatures. The aim of the work described in the present paper was to determine the extent to which the negatively buoyant jet exchanges heat with the surrounding warmer gas and also the extent to which it falls in the motor compartment.

The modelling described in this work makes use of the finite element formulation of the time averaged equations of energy, momentum and turbulence solved within the framework of FEAT [3]. This is a well established method [4], [5], [6] and [7], ideally suited for the calculation of conjugate heat transfer problems, where the equations of transport of heat in a solid and fluid are solved in a close coupled manner with the equations of flow and turbulence in the fluid. The turbulence closure equations are formally κ–ε (Launder – Sharma [8]) although they are actually implemented in terms of primitive variables '*q*' (turbulence speed) and '*f*' the frequency of energy carrying eddies. The equations of transport in the fluid may be solved without reliance on a Boussinesq approximation.

The paper describes the results of one instance of the analysis of the negatively buoyant flow stream injected into the motor compartment. These confirm that, as expected, a coherent stream of cold gas tends to sinks towards the bottom of the compartment, before being drawn into the body of the motor. Interestingly, the details of the results were found to be more sensitive to the prescription of the boundary conditions at the outlet of the domain than to the use or otherwise of a Boussinesq approximation. In practice, such a costly calculation may be used only to justify judgments concerning the high probability of obtaining a coherent stream of cold fluid. These judgments informed the host of simpler analyses actually used to quantify the risk posed to vulnerable non-metallic components as a result of exposure to cold gas. The probability of thermal cycling, arising from an unstable flow distribution was considered, but no attempt to model thermal cycling was undertaken.

As discussed in the text, it was considered that the turbulence modelling had not been tested sufficiently in situations where the density gradients and gravity are aligned, i.e. under stratified conditions. For that reason, a benchmark study involving this very situation was undertaken. The benchmark study was carried out against the experiment of Uittenbogaard [1] on the measurement of turbulent fluxes in stably stratified saline streams. The results of the benchmark study show that the modelling replicates the experimental results over a significant portion of the calculational domain (up to 9 times the channel depth) although after that it is found to overpredict the extent of the mixing between the two streams. In addition, the two equation modelling compares well with similar benchmark studies of the same experiment undertaken with higher order turbulence schemes [2].

Description of plant operation

The design of the gas cooled reactor consists of a reactor and primary circuit wholly contained within a concrete pressure vessel. The primary coolant is pressurised CO_2, which is forced to flow round the primary circuit by electrically powered gas circulator units (pumps). These are housed

within cylindrical penetrations in the side wall of the vessel and consist of large electrical induction motors driving centrifugal impellers. A significant amount of heat is generated in the circulator motor, which requires the rotor and stator to be cooled. This is achieved by forcing CO_2 in the motor compartment to flow through the body of the motor into coolers before being recirculated towards the impeller end by flowing past the outside of the stator. At the impeller end, the CO_2 encounters a fan, which forces the gas back through the body of the motor (Figure 1).

The internals of the gas circulator are not segregated from the primary circuit, to which it is connected through small engineered passages around the bearings. This ensures a controlled net gas flow through the circulator from the reactor outwards into bearing oil drains. Thus, the motor compartment is within the pressure boundary and the conditions of the gas in the primary circuit will be rapidly replicated within the motor compartment, which could mean moist gas entering the motor compartment. Purging has been suggested as a suitable counter-measure for such an eventuality.

The purge gas would be injected into the annular passage at a `top dead centre' location into the annulus formed by the outside of the motor stator and the lining of the penetration housing the unit. This annulus is far from having a uniform cross section, but it will assumed to be so for the purposes of the analysis. The delivery of the purge gas would use existing plant and may not be controlled as accurately as it would be desirable. The delivery system is such that the gas is expected to undergo an isenthalpic expansion from 298K at 40 bar to the conditions reigning within the circulator, which could mean temperatures as low as 241K if the pressure is atmospheric. The purge gas, whether injected as a slug or continuous stream, will join the annular flow but not mix immediately with it. The expectation is that, being a much denser fluid, the purge gas will attain a trajectory consisting of forward motion and a drift towards the bottom of the annulus. All this time the purge gas and the gas already in the annulus will exchange momentum and heat, unless the purge gas reaches the bottom of the annulus where, due to stable stratification, mixing of the two fluids could well cease. It is therefore possible that very cold gas could be drawn into the electric motor.

Metallic components are unlikely to be affected by being bathed in a cold gas stream mainly because a combination of conduction and thermal inertia should mitigate the temperature change. On the other hand non-metallic components, such as electrical insulation of the windings, could suffer, as the outer layers of any coating would attain a low temperature and suffer a significant reduction in life.

Description of numerical modelling

The behaviour of the gas in the motor compartment will be modelled by solving the 'Reynolds averaged Navier Stokes' equations invoking the concept of eddy viscosity to represent the effect of velocity correlations with order higher than 2 ([5], [6] and [7]). This contains the inherent assumption that the turbulent fluctuations in the flow can be regarded as statistically stationary and that the introduction of the purge flow does not alter the statistics significantly.

The eddy viscosity is obtained from the Launder-Sharma turbulence model, with the required closure transport equations formulated in terms of the turbulence speed q and the frequency of large eddies f [3]. Thus, the system of equations solved for the main flow variables, in addition to the conservation of mass embodied in $\nabla.\rho u = 0$, is

$$\rho\frac{\partial u}{\partial t} + \rho u.\nabla u = -\nabla p + \left(\rho - \rho_{ref}\right)g + \nabla\left[\left(\mu + \mu_t\right)\nabla u\right] \qquad (1)$$

$$\rho C_p\frac{\partial T}{\partial t} + \rho C_p u.\nabla T = \nabla\left[\left(k + k_t\right)\nabla T\right] \qquad (2)$$

where μ_t and k_t are the turbulent viscosity and conductivity arising from the modelling of higher order correlations using a scalar coefficient and a velocity gradient. The corresponding diffusivities

are v_t and ε_t .

The turbulent diffusivities are obtained from $v_t = ql$ and $k_t = C_p v_t / \sigma_t$, where q is the turbulence speed, defined as $q = \sqrt{k}$, l is the (Prandtl-Kolmogorov) length scale obtained from $l = C_\mu q / f$ and σ_t is the turbulent Prandtl number for heat transport (set to 0.8 in κ-ε models).

Concentrating on the closure equation for the turbulence speed q,

$$2\rho\frac{\partial q}{\partial t} + 2\rho u.\nabla q - 2\nabla.(\mu\nabla q) - \nabla.\left(\frac{\rho f_\mu l}{\sigma_k}\nabla k\right) = f_\mu l\rho(S_u + S_g) - \frac{2}{3}\rho q\nabla.u - \rho C_\mu\frac{k}{l} + 2\mu\rho\frac{l}{\sigma_k}(\nabla q.\nabla q) \quad (3)$$

The model contains terms particularly relevant to the present analysis. The term $S_g = \frac{-1}{\rho\sigma_T} g.\nabla\rho$ corresponds to the energy exchange between the turbulence field and the gravitational field. It is worth remarking that the calculation of buoyancy influenced flows using eddy viscosity (two equation) models tends to be restricted to flows in vertical channels, precisely because of the difficulty of dealing with turbulence suppression/generation in a stratified flow. In such cases $\nabla\rho$ has only a small component aligned with the gravity vector. Thus this term is expected to be much more significant in the calculation of a flow in a horizontal passage. In particular it can be envisaged that as the cold stream begins to sink along the side of the passage, turbulence will be suppressed along the 'upper' part of its envelope and augmented along the `lower' part of the envelope.

The transport equation for `f', the frequency of the energy carrying eddies, noting that $\varepsilon = q^2 f$.

$$\rho\frac{\partial f}{\partial t} + \rho u.\nabla f - \nabla.(\mu\nabla f) - \nabla.\left(\frac{C_\mu\rho f_\mu q^2}{2\sigma_\varepsilon}\nabla F'\right) = C_\mu f_\mu\rho(C_{1\varepsilon} - 1)(S_u + S_g) - \rho(f_2 C_{2\varepsilon} - 1)f^2 + R_{f\varepsilon} + C_{E\varepsilon}E_f \quad (4)$$

The term S_g is also present in the transport equation for 'f' so that in qualitative terms it can be stated that the dissipation rate will also be suppressed over the 'upper' interface of the cold stream and augmented over the lower interface.

Perhaps the most important effect to be observed is that there will probably be significant attenuation of velocity fluctuations normal to the interface when turbulence generation is suppressed and an enhancement when the generation is augmented. Thus, turbulence is likely to be anisotropic around the interface of the stream. It is worth keeping in mind that an eddy viscosity approach inherently assumes isotropy. Wall functions are used to span the region of the wall up to y^+ of 10-30 in order to reduce the computational effort. In the present work walls are adiabatic thus lessening the risk involved in using wall functions.

The problem has also been addressed using a prescribed length scale and dispensing with the transport equation for the frequency of the eddies. The prescribed length scale assumes the length scale obtained for fully developed turbulent flow in an annulus ($\ell = yC_\mu^{1/4}\kappa$). This is expected to 'smooth' out the rates of turbulence generation around the stream.

The domain consisted of one half of a simple annular passage with smooth adiabatic walls, 1m long and with internal diameter 0.8m and external diameter 1.14m. The mesh consisted of between 20

and 30 layers of elements in a streamwise direction, up to 33 layers azimuthally (with higher density near the top dead centre) and 9 layers in a radial direction with a higher density towards the walls.

One of the great advantages of solving it within the finite element formulation is that the method is 4^{th} order accurate, and any shortfalls in the meshing manifest themselves as 'wiggles' in the solution thus aiding the refinement of the mesh.

Boundary conditions of purge flow

Boundary conditions are key to defining the problem adequately. Notwithstanding that, this aspect tends to be the most problematic part of the analysis and this case is no exception. There are two main uncertainties arising from the complexity of the problem.

Firstly, the exact conditions of injection of the purge flow are unknowable. A jet of cold CO_2 enters the main annular passage, possibly at critical conditions. There is no way of knowing the shape or the velocity profile of the jet. In the present case it is assumed that the purge flow miraculously appears at the inlet plane (cf Figure 1) of the calculational domain with no radial or tangential velocity components and with a flat temperature profile of 265K, while the remainder of the cross section is at 323K. The axial velocity, turbulence and length scale profiles in the inlet plane is assumed to be that of fully developed hydrodynamic flow in an annular passage ($Re \sim 3 \times 10^5$). Clearly, this is a significant simplification, but sensitivity studies indicated that this prescription retained a conservative margin in respect of predicting the mixing of the cold fluid into the surrounding warmer fluid flow.

Secondly, being an elliptic problem, the nature of the conditions specified at exit determine the solution throughout the domain. In reality, the flow beyond the outlet plane (cf Figure 1) of the calculational domain in effect enters a chamber from which it flows radially inwards being drawn by the impeller. The present analysis has not attempted to deal with this complex flow and merely resorts to two simple specifications of conditions at the outlet

1. An outlet plane with no traction forces on the flow, or
2. an outlet plane with a large loss coefficient in the momentum equation

Either is attractive as it requires no specification of a complex tensor and are much better than any assumption of periodic boundary conditions since the presence of a significant buoyancy term will affect the velocity profiles at exit. The disadvantage of the first condition is that this is similar to an open ended passage opening into an infinite environment where the fluid is at a uniform density (ρ_{ref}); in addition this may encourage the denser gas to sink down faster than it otherwise would.

Less obvious but perhaps just as important, symmetry boundary conditions are specified on the mid-plane in order to save computational power. This forces the purge flow to divide symmetrically about the vertical mid-plane, which may well be the most unlikely flow pattern.

The inner and outer surfaces of the cylindrical passage are assumed to be smooth and adiabatic.

Results and discussion of analysis of purge flow

Figure 2 to Figure 5 show the predicted gas temperature maps at the domain outlet for four different variants of the analysis. In all cases the cold stream is shown to be quite coherent and to flatten out as a result of stratification as it begins to sink in the forward motion of the gas. For the specific purposes of the design assessment of the plant modification, there is no essential difference between the variants as they predict that the minimum temperature in the purge flow stream will have risen from 265K to 294-297K after 1m. A closer look reveals substantial differences between the results obtained with the different variants of the analysis. Calculations with a Boussinesq approximation (Figure 2) shows that the core of the stream has sunk less than for the equivalent calculation with variable properties (Figure 4). Figure 3 shows how prescribing a length scale yields apparently reasonably looking results; a detailed scrutiny shows steeper gradients and arguably a reduced rate of spread possibly due to underestimating turbulent mixing. The thermal gradients on the

lower part of the cold stream are predicted to be steeper for the variable property variants (Figure 4 and Figure 5).

Considering the issue of boundary conditions at outlet, the calculations giving rise to Figure 4 differ from those giving rise to Figure 5 in that the former treats the flow at outlet as if it were fully developed, whereas the latter specifies an exit loss equivalent to several dynamic heads. The temperature contours differ quite significantly and it should come as no surprise that plots of the velocity vectors at outlet show the direction of the flow turning sharply downwards. This was true of both variants and clearly highlights a shortfall in the modelling in terms of the prescription of boundary conditions.

The results supported judgments informing a host of simpler calculations carried out to estimate the extent of mixing of a cold purge stream. These estimates entered a design assessment supporting the modification to the plant. This assessment takes into account the hazard posed by the thermal cycling of non metallic components, as these are bathed by a flow where the temperature may vary between 294K and 323K, together with the expected frequency of such an event. Thus it was possible to quantify the risk to the component. The calculations reported here provided evidence that the stream of cold gas is very coherent and that raising the concern was justified in the first place.

Figure 6 shows the development of the 'turbulent conductivity' or 'turbulent transport coefficient of transport for heat' as the flow progresses along the annular passage. This plot highlights the main difference of the use of variable properties, because at inlet the turbulent diffusivity is that of a fully developed flow in an annulus which would not show the peak. The peak is a result of the density difference between the purge flow and the main flow.

Figure 7 shows how the temperature contours develop along the domain; the purge flow 'flattens out' but does retain its coherence. It is also intended to highlight the point that there is very little numerical diffusion in the calculation.

There is no guarantee that the solutions obtained provide an accurate (as opposed to precise) picture of the likely behaviour of the cold purging stream. All the solutions obtained look quite plausible, whether obtained using a crude model such as the q-l or a more accurate one such as the κ-ε, variable or constant properties or alternative exit boundary conditions. This highlights the need for benchmarking, which is the subject of the next section.

Benchmark – Results and discussion

The experiment on a stably stratified flow by Uittenbogaard [1] and the CFD analysis of that experiment by Kidger [2] provide a useful benchmark for the methodology adopted above. The particular experiment concerns the stable stratification resulting from the mixing of two streams with different salinities, where the less dense stream is above the denser stream. Mixing between the two streams is inhibited by the suppression of turbulence by the buoyancy gradient. The actual experiment consisted of an open channel flow in a long channel with smooth bottom and side panels 60m long, 1m wide and 0.56m deep (Figure 8). Two water streams of different salinities separated by a splitter plate came together at the downstream edge of the splitter plate, the beginning of the test section. The researchers made measurements of density, mean velocity, the cross correlation of the instantaneous velocity components, density flux and density variance. The measurements of velocity, density and Reynolds stress made at measurement station at the edge of the splitter plate (0m), became the boundary conditions for the analysis. Kidger [2] used 2nd order turbulence closure equations additionally refined with the 'two component limit' (TCL) model to deal with the anisotropy of turbulent fluxes of momentum resulting from the presence of a wall or a free surface. This approach was found to deal satisfactorily with stably stratified flows as well as free surface jets and in general one would expect the higher order closure schemes to provide a more accurate picture of flow phenomena albeit at the cost of increased computational effort.

The experiment has been modelled using a 2-Dimensional solution of the coupled equations of momentum and salinity transport in the framework of a variable property formulation. The closure

equations are provided by the transport equations of turbulence speed 'q' and eddy frequency 'f' again making use of the κ-ε model (Launder-Sharma). Note that in this framework, turbulent fluxes are not modelled and can only be inferred from the two equation model. The domain consisted of a rectangle 0.56m wide ('depth') and 60m long. The meshing along the depth of the passage consisted of 50 finite elements of variable width, so that the mesh density was larger near the bottom wall and the interface of the two streams. No particular care was taken with the top surface, which was merely modelled as a slip surface. The length of the domain was covered with up to 600 elements. In reality, the overall quality of the solution was insensitive to the number of streamwise elements beyond about 200-300. The use of a larger number was an attempt to remove oscillations feeding back into the domain from the outlet plane.

The results of the benchmark study show a reasonably good agreement between the experiment and the current predictions of streamwise velocity, relative density and the turbulent velocity cross correlation $\overline{u_1 u_2}$ at the 5m measurement station. (Figure 9, Figure 10 and Figure 11). By the 10m measurement station, the agreement between predictions and measurements of velocity and relative density has deteriorated somewhat. The predicted distribution of the cross correlation has diverged significantly from the measurements. There is no agreement between the current predictions and experiments by the 40m station.

As expected, the predictions obtained in [2] from higher order turbulence closure are somewhat better, although even for these agreement is very poor after the 10m station (Figure 13, Figure 14 and Figure 15). It is arguable that the good agreement between the present study and the previous experimental and numerical study show that that the restriction to a 2 dimensional analysis is not critical for short distances downstream from the inlet.

Notwithstanding the shortcomings highlighted, the two-equation turbulence model performed quite well over a small but significant span of the experiment and arguably as well as the higher order model. This provides confidence that the methodology is sound even if it is necessary to restrict its scope of application.

Acknowledgement

The author gratefully acknowledges the permissions granted by Dr R Uittenbogaard from Delft University to use his original material, and Prof. B E Launder from the University of Manchester to use original work published by the University. There is a debt of gratitude to Dr J Kidger for the help given to reproduce his plots. Thanks are due to British Energy Generation Ltd for their permission to publish material produced with FEAT and inspired by analysis work undertaken within Engineering Division.

Nomenclature

C_p	Specific heat capacity at constant pressure (J/kgK).
Cμ	Ratio of turbulent shear stress to kinetic energy in simple shear (production=dissipation) =0.09
f	Frequency of large scale eddies (s^{-1}), defined by $\varepsilon = q^2 f$
F	$ln f^2$
g	Gravity acceleration vector.
q	Turbulence speed (m/s). $q = \sqrt{k}$
u	Flow velocity vector (m/s).
T	Temperature (or relative density after suitable normalisation)

ε_t	Turbulent heat diffusivity (m^2/s).
κ	Conductivity (W/mK) plus one instance of the v.Karman constant (for the law of the wall).
κ_t	'Turbulent' conductivity (W/mK), defined by $\rho C_p \overline{u_i \theta} = \kappa_t \nabla T$.
ℓ	Prandtl-Kolmogorov length scale (m)
μ	Dynamic viscosity (Kg/ms).
μ_t	Eddy viscosity (Kg/ms).
ν	Kinematic viscosity (viscous momentum diffusivity) (m^2/s).
ν_t	Turbulent momentum diffusivity (m^2/s).
ρ	Density (kg/m^3).

References

1. R Uittenbogaard, '*Measurement of turbulent fluxes in a steady, stratified mixing layer*', 3rd Int Sym on Refined Flow Modelling and Turbulence Measurements, Tokyo 1988, pp 725-732
2. J Kidger, '*Turbulence modelling for stably stratified flows and surface jets*', UMIST, Ph D Thesis, 1999, TFD/99/07
3. '*FEAT User Guide Version 3.7.1*', published on behalf of BEGL, 2005
4. R M Smith, '*Finite Element Solutions of the Energy Equation at High Peclet Number*', Computers and Fluids, Vol 8, pp 335-350, 1980.
5. R M Smith, '*A Practical Method of Two-Equation Turbulence Modelling using Finite Elements'*, Int. Jou. for Numerical Methods in Fluids, Vol 4, 321-336, 1984.
6. R M Smith, '*On the Finite-Element Calculation of Turbulent Flow Using the κ-ε Model*', Int. Jou. for Numerical Methods in Fluids, Vol 4, 303-319, 1984.
7. A G Hutton, R M Smith and S Hickmott, '*The Computation of Turbulent Flows of Industrial Complexity by the Finite Element Method – Progress and Prospects*', Int. Jou. for Numerical Methods in Fluids, Vol 7, 1277-1298, 1987.
8. Launder, B. E. and Sharma, B. I., '*Application of the Energy-Dissipation Model of Turbulence to the Calculation of Flow Near a Spinning Disc'*, Letters in Heat and Mass Transfer, Vol. 1, pp. 131—138, 1974

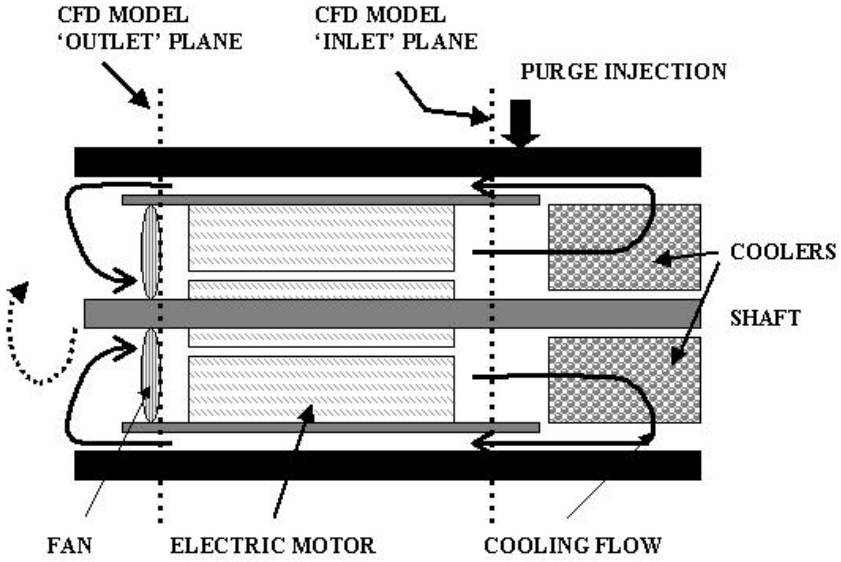

Figure 1: Outline of circulator unit

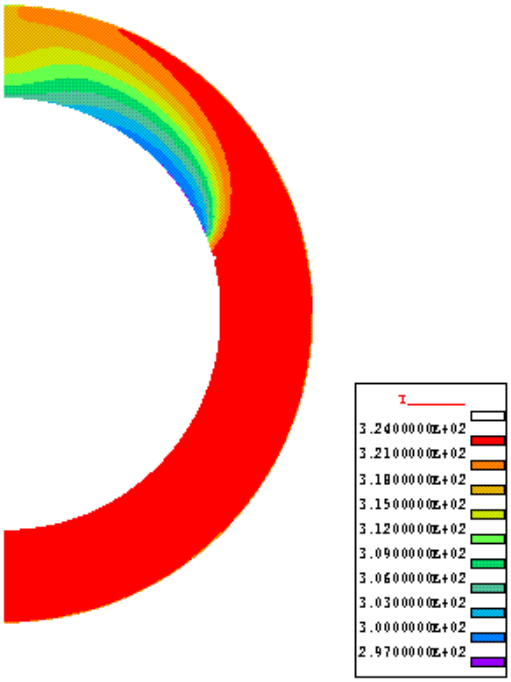

Figure 2 - Temperature contours - Boussinesq- κ-ε (LS) – semi traction at outlet (297K-324K)

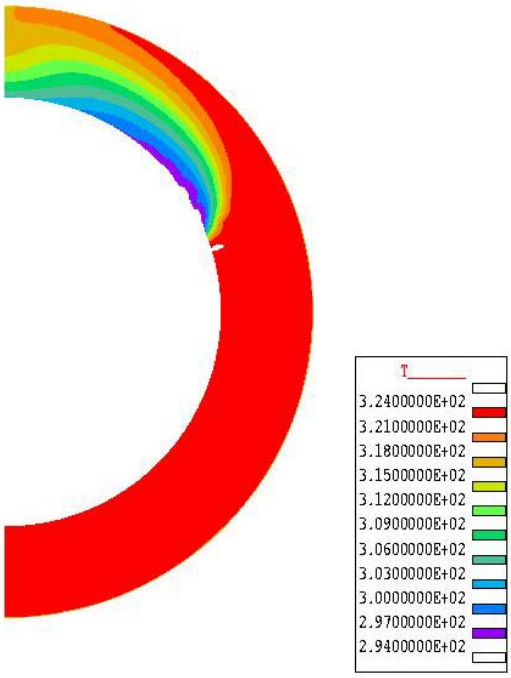

Figure 3 – Temperature contours – (Boussinesq) - q-l –semi traction at outlet (294K-324K)

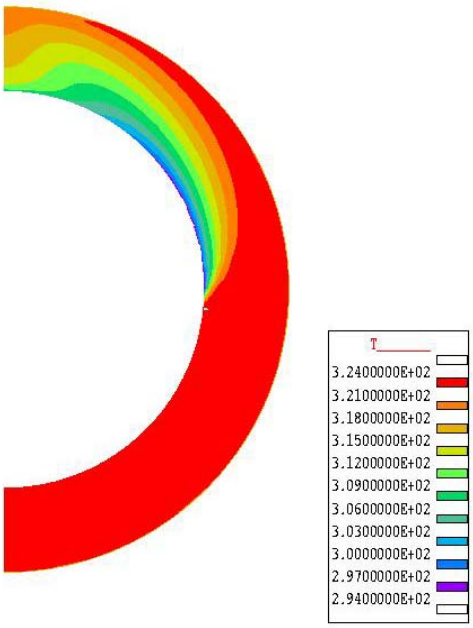

Figure 4 - Temperature contours – variable property- κ-ε (LS) semi-traction at outlet

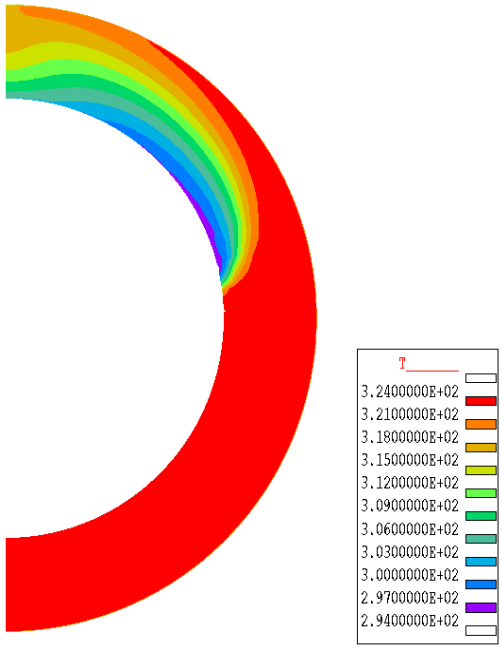

Figure 5: Temperature contours – variable property- κ-ε (LS) exit loss at outlet (294K-324K)

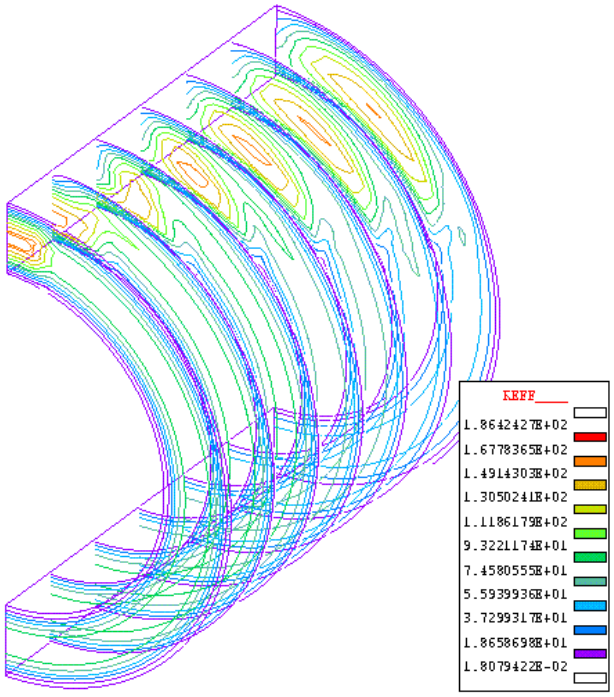

Figure 6: Contours of effective conductivity (0.018-186.4 W/mK)

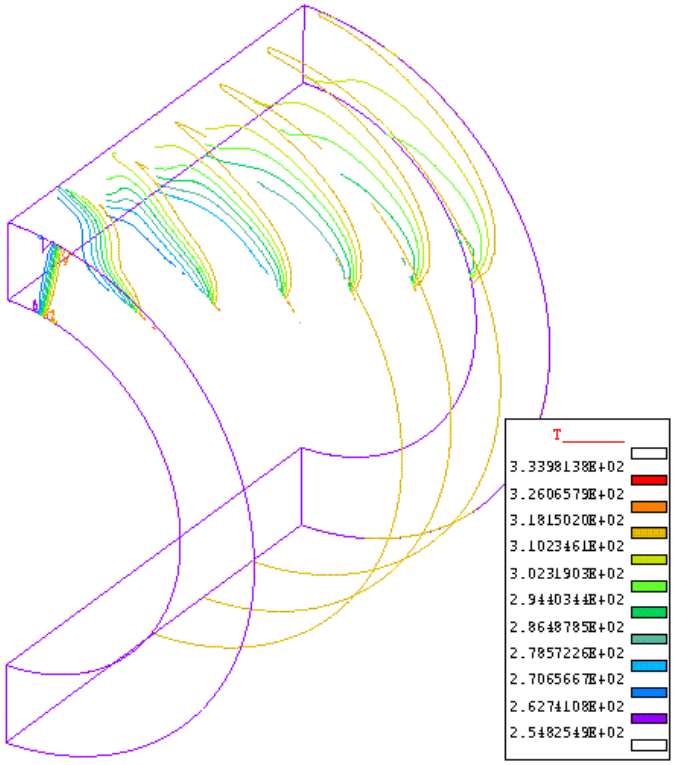

Figure 7 : Contours of temperature (254.8K- 334.0K)

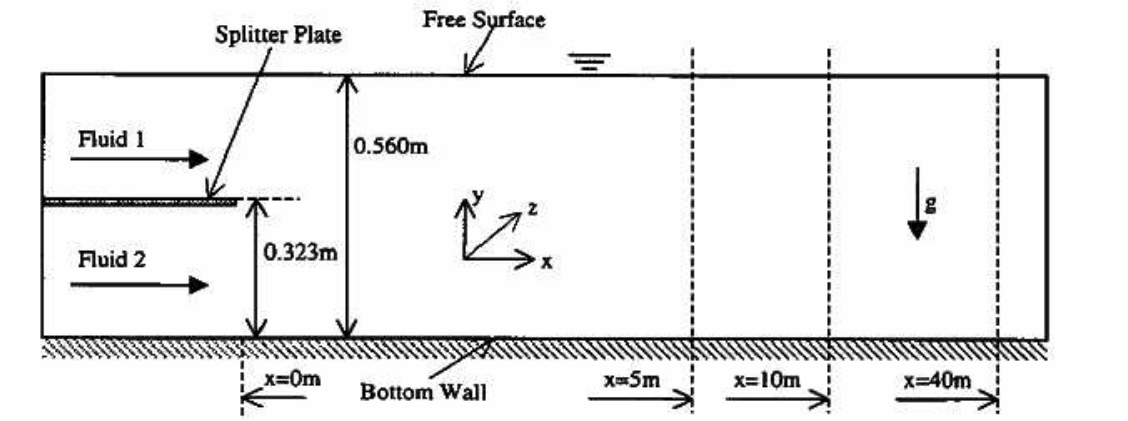

Figure 8: Schematic of experimental geometry

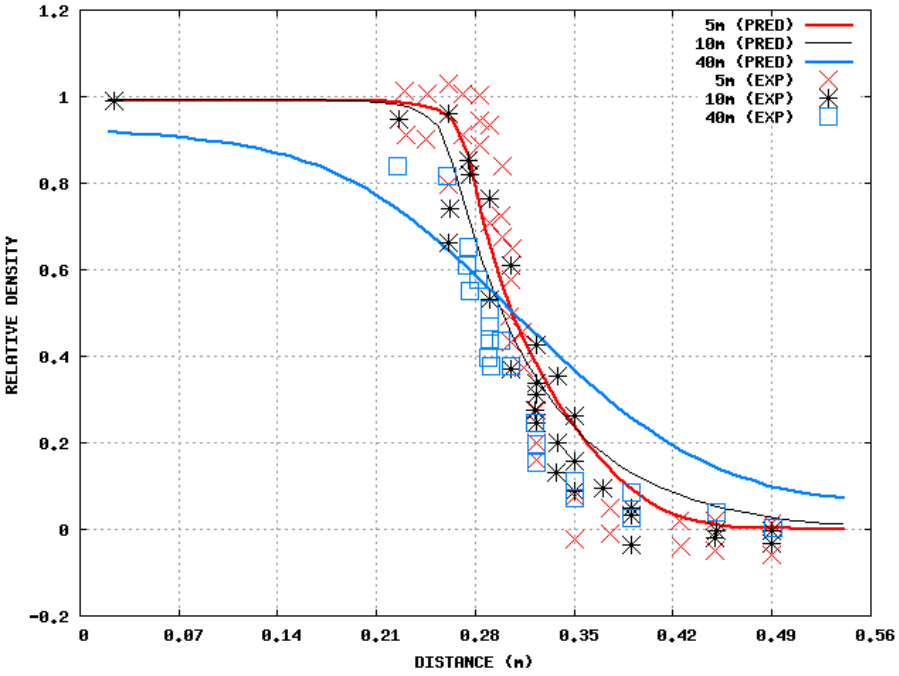

Figure 9: Relative density - Current predictions and experimental results

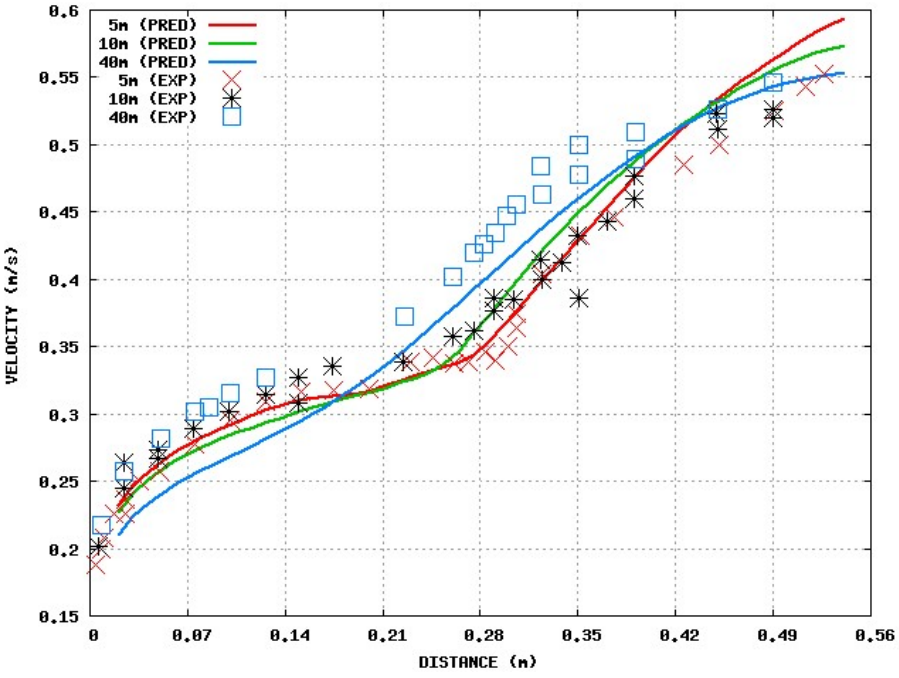

Figure 10 : Streamwise velocity – current predictions and experimental results

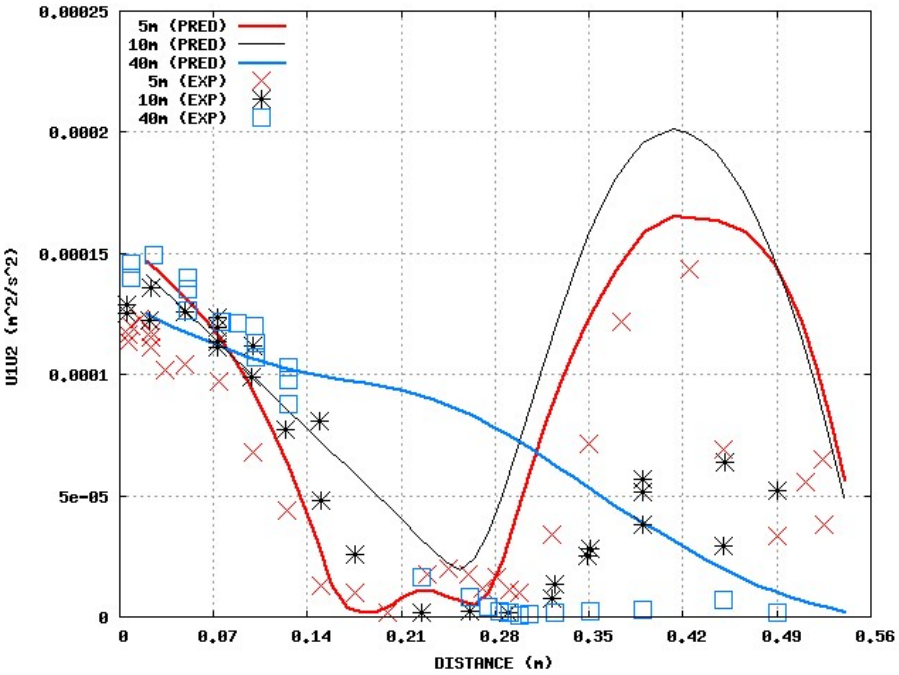

Figure 11 : Cross correlation of velocity components. Current predictions and experimental results

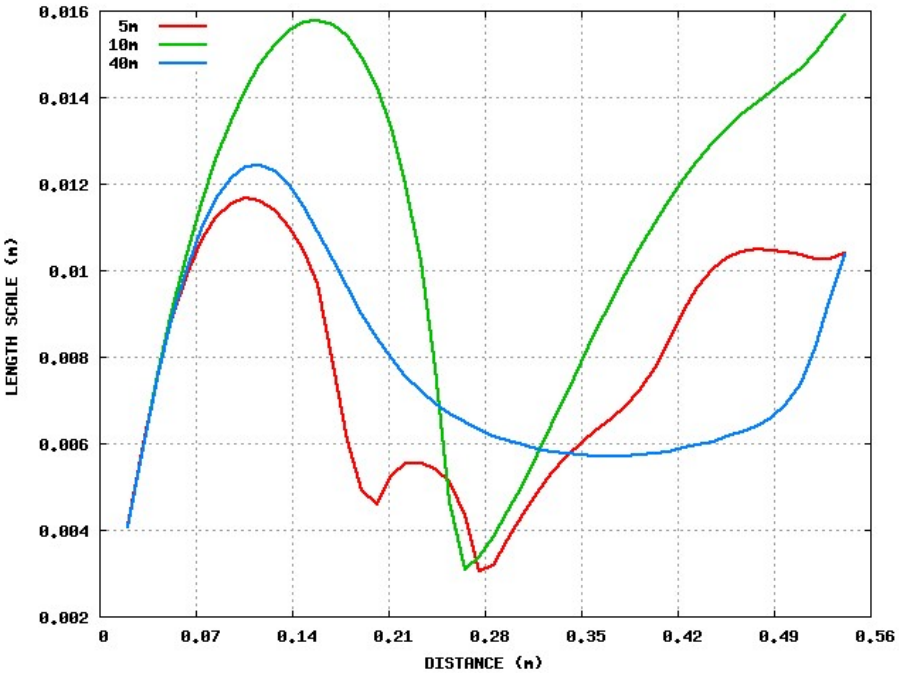

Figure 12 : Prandtl- Kolmogorov length scale - current predictions

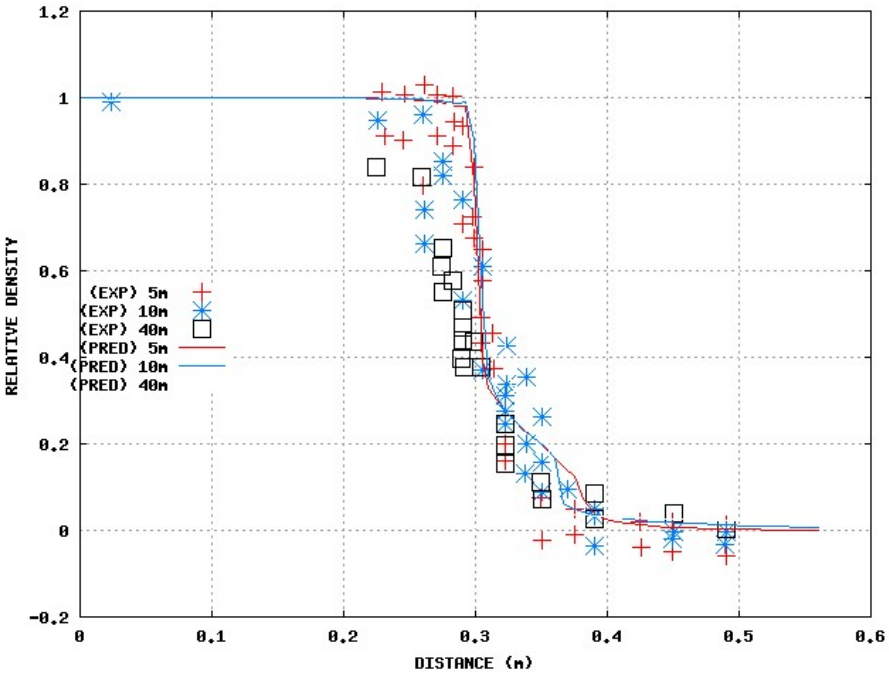

Figure 13: Relative density (Kidger)

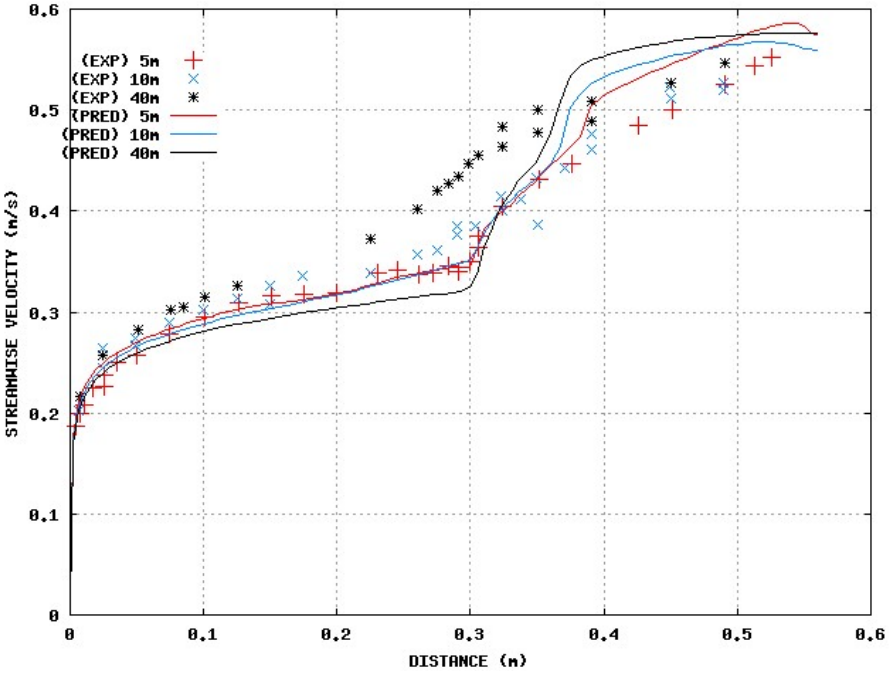

Figure 14: Streamwise velocity (Kidger)

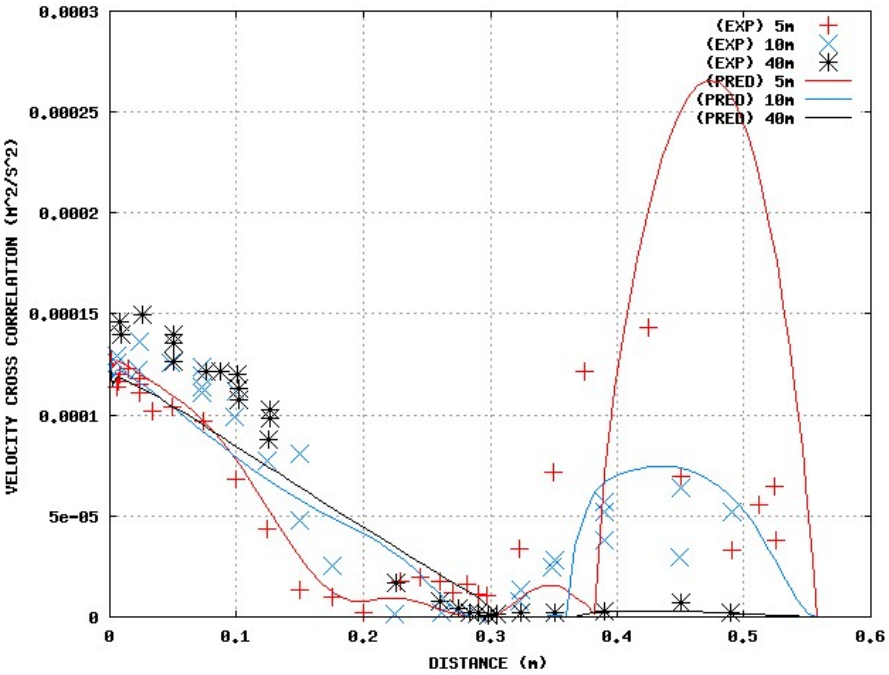

Figure 15: Turbulent velocity cross correlation (Kidger)